Segregations in clusters of galaxies[*]

C. Adami[1]**, A. Biviano**[2]**, and A. Mazure**[1]

[1] IGRAP, Laboratoire d'Astronomie Spatiale, Traverse du Siphon, F-13012 Marseille, France
[2] Istituto TeSRE, CNR, via Gobetti 101, I-40129 Bologna, Italy

Abstract. We analyse a sample of about 2000 galaxies in 40 regular clusters, to look for evidence of segregation with respect to galaxy luminosities and morphological types.

We find evidence of luminosity segregation for galaxies brighter than $M_R < -21.5$, i.e. typically the four brightest members of each cluster. We also find evidence of morphological segregation: both the core-radius and the velocity dispersion increase along the Hubble sequence (ellipticals - S0 - early spirals - late spirals).

Galaxies of different types have different velocity dispersion profiles, being steeper for later type galaxies. Simple modelling allows us to show that elliptical (and, to a lesser extent, S0) orbits are mostly tangential in the cluster core, and nearly isotropic outside, while spiral (in particular late-spiral) orbits are predominantly radial.

A viable interpretation of our results is that (1) late spirals, at variance with other type galaxies, are a non-virialized cluster population, still on partially radial infalling orbits, (2) the elliptical phase-space distribution is evolving towards energy equipartition through the process of dynamical friction, (3) S0 and early-spirals have intermediate distributions between these two extremes.

Key words: galaxies: clusters: general-cluster: individual: Coma cluster

1. Introduction

The analysis of the phase-space distributions of cluster galaxies helps to constrain models of galaxy formation and evolution. In particular, it is important to distinguish among galaxies of different luminosities and morphological types, as they may not have formed and evolved in the same way. Moreover, it is important to know the phase-space distributions of different cluster galaxies for a proper determination of the cluster mass (Girardi et al. 1996).

The observational evidence that early-type galaxies occupy denser environments than late-types dates back to Curtis (1918) and Hubble & Humason (1931), and was quantified by Oemler (1974). Melnick & Sargent (1977) showed that the relative fraction of S0 and spiral galaxies depends on the distance from the cluster centre. Most subsequent studies were based on the data sample of Dressler (1980a) containing over 6000 galaxies in 55 cluster fields. While Dressler (1980b) concluded that the basic correlation is between morphology and *local density* in clusters, Sanromà & Salvador-Solé (1990) and Whitmore & Gilmore (1991), based on the same sample, have independently reached the conclusion that the fundamental correlation is between morphology and *global cluster properties,* such as the the clustercentric distance. For more complete reference, we refer the reader to Whitmore et al. (1993).

More recently, ellipticals and S0 were found to have smaller velocity dispersions (σ in the following) than spirals and irregulars (Tammann 1972; Melnick & Sargent 1977; Moss & Dickens 1977; Sodré et al. 1989; Biviano et al. 1992, hereafter B92; Andreon (1996); Stein 1997, hereafter S97). As morphologies are usually more difficult to reliably determine than colours, and colours and morphologies are correlated, many authors have analysed the correlation between kinematics and colours. Biviano et al. (1996), Colless & Dunn (1996), all found that the ratio between the σ of the blue and the red galaxy populations in the Coma cluster is ~ 1.3–1.4. Similar evidence has recently been found by Carlberg et al. (1997) in their analysis of the CNOC survey medium-z clusters. Based on a sample of ~ 600 galaxies in 15 clusters, S97 has recently confirmed the larger σ for spirals as compared to early-type galaxies, and has shown that within the class of early-type galaxies, S0 have a larger σ than ellipticals.

Further, possibly related, observational evidence is the existence of luminosity segregation: the most luminous galaxies are closer to the cluster centres (e.g. Rood & Turnrose 1968, Capelato et al. 1981, Yepes et al. 1991), and have a significantly lower velocity dispersion (Rood et al. 1972, Chincarini & Rood 1977, Struble 1979, Kent & Gunn 1982, B92, S97). The anti-correlation between luminosity and velocity dispersion seems however to hold for the very bright galaxies only (luminosity $\geq 5L^\star$), and to depend on the galaxy morphological type, being

strongest for ellipticals (B92, S97). S97 in particular has pointed out that there is no evidence whatsoever for a σ–luminosity (anti-)correlation in galaxies other than ellipticals.

Only very recently, large data-sets have allowed the analysis of the velocity dispersion profiles (*vdp* in the following) of galaxies of different properties. Mohr et al. (1996) have shown that the emission-line galaxies in the A 576 cluster have a steeper *vdp* than non-emission-line galaxies; Biviano et al. (1997, hereafter B97) have come to the same conclusion on the basis of the ENACS data-set of 75 clusters (see Katgert et al. 1996, hereafter K96). A similar difference is found between the *vdp* of red and blue galaxies in 15 clusters from the CNOC survey (Carlberg et al. 1997).

From the theoretical side, the evidence for segregation is interpreted either as arising in a different formation process for galaxies of different luminosities and/or morphologies, or as being due to a different evolutionary history (the "nature vs. nurture" problem). Many physical processes can affect the morphology, luminosity, and velocity of a galaxy. Dynamical friction can slow down the more massive galaxies, circularize their orbits (den Hartog & Katgert 1996 and references therein), and enhance their merger rate (Mamon 1992, 1996 and references therein); ram pressure and collisions can transform a star forming galaxy into a quiescent one; tidal effects can truncate the galaxy sizes and reduce their luminosities while producing a reservoir of debris for centrally located cD galaxies (Oemler 1992, Whitmore 1994, and references therein). The steep *vdp* and large σ of star-forming galaxies, as compared to quiescent ones, suggests that star-forming galaxies are falling into the cluster, maybe for the first time (B97).

In this paper we revisit these issues, via the analysis of a large data-set of about 2000 cluster galaxies, partly based on the ENACS catalogue (K96, Katgert et al. 1997), and partly drawn from the literature. Taking a step further from previous studies on segregation, we distinguish spirals into two classes (early- and late-type), and determine the *vdp* of ellipticals, S0, early-spirals and late-spirals.

The structure of the paper is as follows: in Sect. 2 we describe the data-sample, in Sect. 3 we address the issues of segregation in velocities and spatial segregation, and determine the *vdp* for different morphological classes; in Sect. 4 we discuss our findings, and in Sect. 5 we give our conclusions.

2. The data

2.1. The compilation of the catalogue

The data sample on cluster galaxies which we use in this paper is a merging of the ENACS data-base (K96 and Katgert et al. 1997) and available data from the literature, which includes the December 1994 version of ZCAT (Huchra et al. 1995). Coordinates and redshifts are available for all galaxies in our data sample, and magnitudes and morphological types are available for most of them.

In compiling this data-base, we had to make a compromise between collecting as much data as possible, and keeping the data-base homogeneous. For this reason, before putting together data from different sources, we first compared the different redshift estimates for galaxies common to different data-sets. Only when the average velocity difference of all common galaxies was not statistically significant (at the 90 % confidence level) and less than 200 km s^{-1}, were the different source redshift scales considered compatible and the data-sets merged together. For a comparison of ENACS and literature data we refer the reader to K96.

In merging different data-sets, one has to take special care not to insert the same galaxy twice. This may happen if the galaxy coordinates in either of the two data-sets are not accurate enough. For the ENACS clusters, we made use of the (unpublished) catalogue of galaxies obtained by scanning film copies of the SERC blue survey and glass copies of the first Palomar Sky Survey, with the *Astroscan* measuring machine (K96 and references therein). This catalogue was used in preparing the Optopus observations; for all detected galaxies a photometric parameter was derived, which was later converted into an isophotal magnitude (R_{25}) using CCD-observations for calibration (more details are given in K96). This photometric catalogue is meant to be complete, but only for selected cluster regions specifically chosen for the Optopus observations. When a galaxy with a redshift measurement from the literature was located in the Optopus plate cluster regions, it was possible to find a corresponding entry in the *Astroscan* catalogue. If the galaxy already had an ENACS redshift measurement, this was adopted; otherwise, the literature redshift was used, but the coordinates and magnitudes were taken from the *Astroscan* catalogue, for a better consistency with other ENACS galaxies.

For the non-ENACS clusters, or for regions of the ENACS cluster not covered by the Optopus plates, we took a conservative approach and rejected all suspected double entries for the same galaxy. The decision was based upon similarity of coordinates (up to 30" difference), and galaxy properties like redshift, and/or magnitude, and/or morphology. We may have eliminated galaxy pairs, but this is not a concern for the present analysis, as long as the probability for galaxies to be in pairs does not depend strongly on their morphological type and/or luminosities.

The average galaxy velocity uncertainty in our final data-set, using the errors quoted in the original references, is 69 km s^{-1}, and the maximum quoted uncertainty is 276 km s^{-1}. External errors are likely to be larger, due to the non-perfect match of the redshift scales of merged data-sets.

Magnitudes were corrected for galactic absorption, using the extinction-maps of Burstein & Heiles (1982), and the relations between $E(B - V)$ and absorption in several magnitude bands as given by Colless (1989), Oemler (1974), and Postman & Lauer (1995). We applied k-corrections using the relations given by Colless (1989), Postman & Lauer (1995), Sandage (1973), and Schneider et al. (1983). All magnitudes were then converted to ENACS R_{25} magnitudes. When possible, the linear regression between the ENACS and the literature magnitudes for common galaxies was used as a conversion formula. Otherwise, we used relations given in the literature to convert from total to isophotal magnitudes, when needed, and from different

bands to the red bandpass (ref.s mentioned above and: Dickens et al. 1986, Lugger 1989, Oegerle & Hoessel 1989, and Sharples et al. 1988).

The uncertainty of ENACS magnitudes is ≤ 0.3 mag (and even lower for galaxies in clusters with CCD-calibration, see K96). The uncertainty of the magnitudes taken from the literature is probably larger (≤ 1 mag), because of the additional error introduced in transforming them to the ENACS bandpass.

All the morphological type estimates were taken from the literature, as there is no morphological information available in the ENACS data-set.

2.2. The definition of clusters

Several methods have been proposed in the literature for defining cluster membership. As a large part of our data comes from ENACS, it would be natural to follow K96's methodology of fixed gaps: redshift boundaries for a cluster are defined such that the closest non-cluster member in redshift space is separated by at least 1000 km s^{-1} from either of the two boundaries. However, a fixed gap of 1000 km s^{-1} is a valid choice only for the relatively homogeneous ENACS sample, but cannot work for all data-sets, simply because the average density of observed galaxies per redshift interval may change (as a consequence of one survey being deeper than another). As an example, the fixed gap fails to effectively identify the Coma cluster in redshift space.

For this reason, we adopted a gap that depends on the galaxy density per redshift interval along the line-of-sight to a given cluster, and we call it the density-gap, equal to $500 + 600 \exp(-n/33)$ km s^{-1}, where n is the total number of galaxies with measured redshift in the cluster region. This expression was derived from simulations of the occurrence of gaps of a given size in gaussian distributions with varying numbers of objects. When applied on the ENACS data-base it identifies similar systems as those identified using the fixed gap criterion (see also Adami et al. 1997a).

Using the density-gap method we identified the main systems along the lines of sight. For the cluster A 548 alone we also applied a splitting in coordinate space, since it is clearly bimodal in projection (Escalera et al. 1994).

In order to further reject possible remaining interlopers, we then applied the method of den Hartog & Katgert (1996) to the systems with at least 50 galaxies (the method is unreliable for poorer data-sets).

It is important to use only the central regions of clusters in our analysis, in order to minimize spatial selection effects. In denser regions, multi-object spectroscopy – from which most of our data comes – tends to select brighter galaxies than in less dense region. On the other hand, deeper surveys are done with smaller fields of view, which means that the central cluster regions are generally sampled to fainter magnitudes than the wider external regions. While a detailed analysis has shown that these selection effects are of no concern for the ENACS data-set (Adami et al. 1997b), we do need to worry about this issue when using literature data. To reduce this problem, we chose to con-

sider only galaxies within 1 h^{-1} Mpc radius[1] from the cluster centres. Via this selection we also implicitly exclude regions that have not yet reached virialization (e.g. White 1992), yet which inlude most of the cluster galaxies, as their projected density at 1 h^{-1} Mpc is low, being < 8 % of the central density for 80 % of the clusters (Girardi et al. 1995). Centres were defined by choosing the peak of the X-ray emission, when available, or the location of the cD, when present, or else the isodensity contour peak (as in Adami et al. 1997b).

As was shown by Beers et al. (1990), ~ 20 data-points are sufficient to provide robust estimates of the central location and scale of a data-set, when the biweight estimators are used (see also Lax 1985). On the other hand, Girardi et al. (1993) have shown that changing the cluster membership criterion changes the cluster σ estimate if only 10 galaxies per cluster are available. As a consequence, we considered in our analysis only those clusters with at least $\simeq 20$ galaxy members within a circle of 1 h^{-1} Mpc radius (the minimum number of cluster galaxies in our sample is 18, in the cluster A 978).

The final sample contains 2219 galaxy members from 40 nearby clusters (counting the subclusters in A 548 as two independent systems). The mean cluster redshifts range from 0.013 to 0.075; the absolute R$_{25}$ magnitudes of cluster galaxies range from -23 to -16; the morphological fractions of the 1997 galaxies are: 24 % ellipticals (E, hereafter), 49 % S0, 21 % early spirals (Sa to Sb in the Hubble sequence, globally labelled Se, hereafter), and only 6 % late spirals or irregulars (Sl, hereafter). These fractions are similar to the average fractions for all kinds of clusters (spiral poor, spiral rich and cD) as given by Oemler (1974).

In Table 1 we list for each system the cluster Abell number, the number of very bright galaxies (i.e. those with a cD morphology and those separated by a gap of at least 0.5 mag from the fainter galaxies), the total number of redshifts, the mean redshift of the cluster, the clustercentric distance that defines the region analysed in this paper, the velocity dispersion and its bootstrap error based on 1000 resamplings, the type of the selected centre ("I" means the centre was chosen at the isodensity peak, "cD" that it coincides with the position of the cD galaxy, "X" that it coincides with the position of the X-ray peak), and the relevant references to the collected data.

While this paper was being written, the data-set of Stein (1996) on cluster galaxies became available. As this data-set is not included in our compilation, it makes sense to compare Stein's determinations of the cluster parameters with ours. There are five clusters in common with Stein (1996) in our data-set: A 400, A1016, A1060 (Hydra), A3526 (Centaurus) and A4038. As Stein's sample is limited to the inner 0.5 h^{-1} Mpc, we restricted our samples to this inner region as well, for the sake of comparison. We find an average difference of 37 km/s in the σ estimates, and of -122 km/s in the average velocity estimates, both within their 1-sigma uncertainties.

---

[1] Throughout the paper h=H$_0$/(100 $km\ s^{-1}\ Mpc^{-1}$), and the deceleration parameter $q_0 = 0$

Table 1. Parameters for the 40 clusters. The chosen centres are denoted by "X" when they are X-ray determined, "cD" when they coincide with the position of a cD galaxy, "I" when they are chosen at the peak of isodensity contours. We show the number of bright galaxies for each cluster (see text). The references are: A: Adams et al. (1980); B1: Beers & Bothun (1992); B2: Beers et al. (1991); B3: Biviano (1986); B4: Bothun & Schombert (1988); B5: Butcher & Oemler (1985); B6: Biviano et al. (1996) and references therein; C1: Chapman et al. (1987); C2: Chapman et al. (1988); C3: Chincarini et al. (1981); C4: Colless & Hewett (1987); C5: Colless (1989); D1: Dickens et al. (1986); D2: Dickens & Moss (1976); D3: Dressler & Shectman (1988); D4: Dressler (1980a); E: Ettori et al. (1995); F1: Faber & Dressler (1977); F2: Fabricant et al. (1993); F3: Fabricant et al. (1989); F4: Fanti et al. (1982); G1: Gavazzi (1987); G2: Geller et al. (1984); G3: Giovanelli et al. (1982); G4: Gregory et al. (1981); G5: Gregory & Thompson (1978); H1: Haynes (1980); H2: Hill & Oegerle (1993); H3: Hintzen et al. (1982); H4: Hintzen (1980); K: Kent & Sargent (1983); L1: Lauberts & Valentijn (1989); L2: Lucey & Carter (1988); L3: Lucey et al. (1983); M1: Malumuth et al. (1992); M2: Moss & Dickens (1977); N: Nilson (1973) O: Ostriker et al. (1988); P1: Pinkney et al. (1993); P2: Poulain et al. (1992); P3: Proust et al. (1992); Q1: Quintana & Ramirez (1990); R1: Richter (1989); R2: Richter (1987); S1: Scodeggio et al. (1995); S2: Sharples et al. (1988); T1: Tarenghi et al. (1979); T2: Teague et al. (1990); T3: Tifft (1978); W: Willmer et al. (1991); Z1: Zabludoff et al. (1993); Z2: Zabludoff et al. (1990); Z3: Zwicky et al. (1968)

| Name	Bright galaxies	Nb of redshifts	Mean redshift	Extension (h^{-1} kpc)	σ (km/s)	Center	References
A0119	1	73	0.042	994	943±170	I	F2+ENACS
A0151	1	31	0.052	897	804±181	I	D4+P3+ENACS
A0168	1	59	0.044	977	528±80	I	F1+Z2+ENACS
A0194	0	52	0.017	965	523±208	X	C2+B3
A0262	0	40	0.016	996	506±110	X	G3+G4+M2+Z3
A0400	0	69	0.023	909	629±100	X	B1+B5+D4
A0426	0	75	0.017	798	1329±205	X	B3+K+P2+Z3
A0496	1	56	0.033	898	746±153	X	D4+M1+Q1
A0539	0	71	0.029	996	1095±390	X	O+N+Z3
A0548	0	88	0.041	992	736±84	X	D3+ENACS
A0548	0	95	0.042	990	885±79	X	D3+ENACS
A0576	0	26	0.038	670	927±244	X	H1+H3+F4
A0754	1	51	0.056	878	914±186	X	D3+ENACS
A0978	1	18	0.056	992	674±181	I	D4+ENACS
A0999	1	23	0.033	700	393±185	cD	A+C1
A1016	1	22	0.033	575	257±80	cD	A+C1
A1060	2	112	0.013	951	665±78	X	R1+R2
A1142	0	32	0.037	958	441±141	X	B3+D4+G2
A1367	0	50	0.023	863	878±255	X	D2+G1+G5+T3+Z3
A1631	1	43	0.048	996	706±159	X	D3
A1644	1	58	0.049	964	966±201	X	D3
A1656	1	196	0.024	974	1135±127	X	B6
A1983	2	42	0.045	903	593±101	X	D3
A2040	0	25	0.046	796	730±248	X	Z2+ENACS
A2063	1	38	0.035	928	744±199	X	B2+D4+H2
A2147	0	22	0.037	971	1194±401	X	T1+Z3
A2151	0	74	0.037	983	861±122	X	D3
A2256	1	56	0.059	890	1403±221	X	F3
A2634	0	22	0.030	832	938±530	X	B4+B5+D4+H4+ P1+S1+Z1
A2670	2	95	0.075	978	1120±191	X	S2
A2877	1	37	0.023	865	790±376	X	M1
A3128	1	80	0.059	997	1041±162	I	C4+C5+ENACS
A3158	5	33	0.059	778	1064±294	I	C3+L2+ENACS
A3376	1	53	0.047	995	790±163	X	D3
A3381	1	26	0.038	777	306±145	X	D3
A3389	2	37	0.027	585	620±109	X	D3+T2
A3526	0	107	0.013	994	962±93	X	D1+L1
A3574	0	33	0.016	881	513±115	X	W
A3716	0	57	0.044	966	845±117	X	C4+D3
A4038	1	42	0.028	771	872±288	X	E+L3
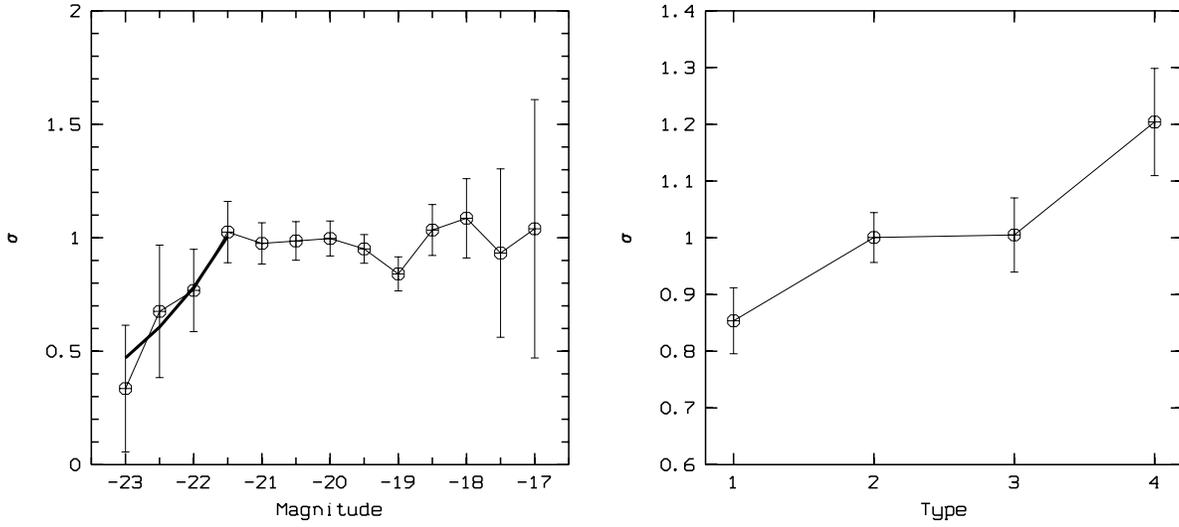
Fig. 1. a (left panel) normalized σ vs. M_R magnitude for all galaxies in the synthetic cluster (1997 galaxies). We show the relation $\sigma \propto 10^{0.2M_R}$, normalized at $M_R = -21.5$; **b** (right panel) normalized σ vs. morphological type for galaxies in the synthetic cluster with 1: E, 2: SO, 3: Se and 4: Sl.
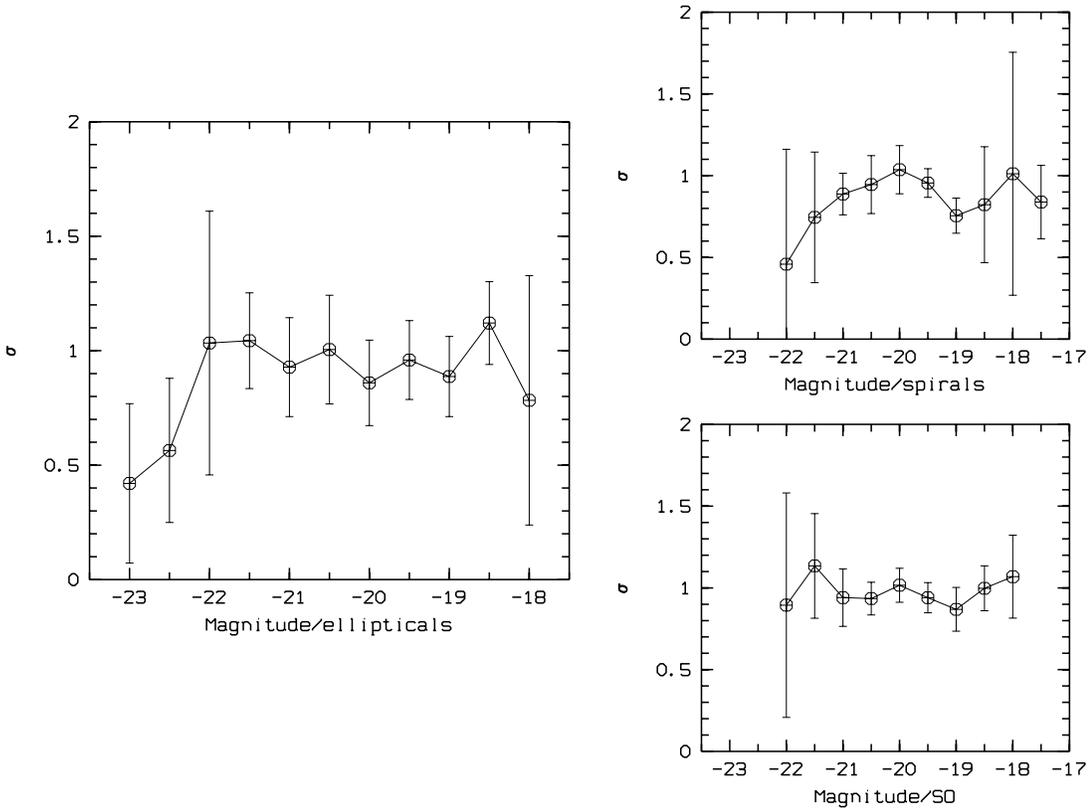

Fig. 2a–c. Normalized σ vs M_R magnitude for the galaxies in the synthetic clusters, split into three morphological classes; **a** (left panel) E (479 galaxies); **b** (bottom-right panel) S0 (982 galaxies); **c** (top-right panel) spirals (536 galaxies).
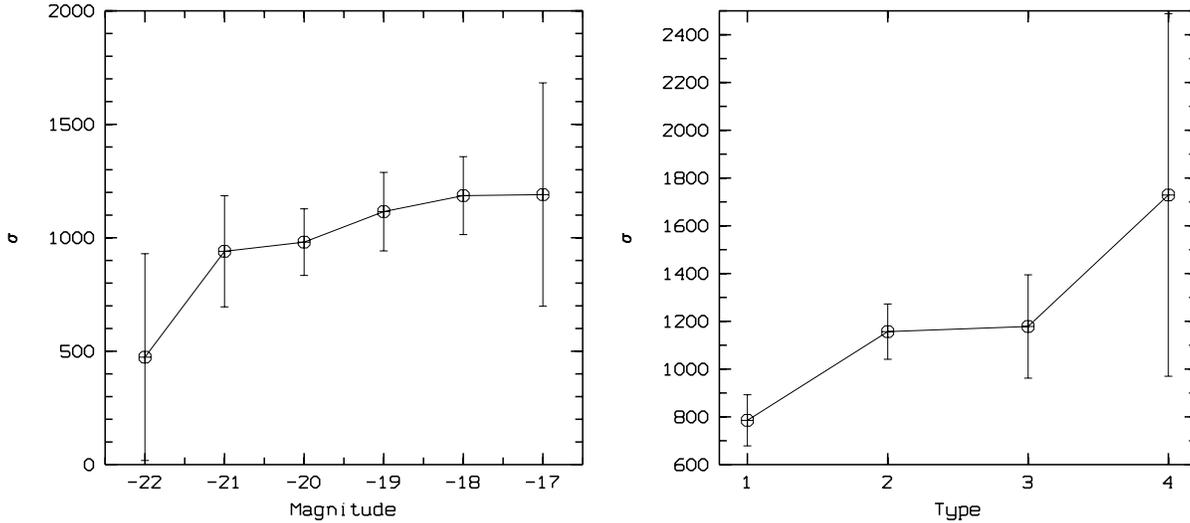
Fig. 3. Segregation in the Coma cluster; left panel: σ (km/s) vs. M_R magnitude; right panel: σ (km/s) vs. morphological type, with 1: E, 2: SO, 3: Se and 4: Sl.

3. Analysis and results

Our results are based on the analysis of a synthetic cluster that we have created by joining all 40 cluster samples (as in B92; see also B97 and S97). In the synthetic cluster, galaxy distances are in unit of h^{-1} Mpc from the centre of the cluster they belong to. Galaxy absolute magnitudes, M_R, are obtained from apparent magnitudes by using the mean cluster distances, and galaxy velocities are referred to the cluster average velocities and scaled by the cluster velocity dispersions,

$$v_i^{(n)} = \frac{v_i - <v>_j}{\sigma_j} \tag{1}$$

where i and j are, respectively, the galaxy and the cluster indices.

In order to check the results obtained on the synthetic cluster, the same analysis was also performed on a single cluster, Coma (A 1656), for which a large enough data-sample was available. The morphological fractions of Coma galaxies are similar to those of the synthetic cluster.

In all following analyses, error-bars are obtained from a bootstrap technique with 1000 resamplings.

3.1. Segregation in velocity

In order to test for the presence of luminosity segregation in velocity space, we have computed the (normalised) velocity dispersion, $\sigma^{(n)}$, of the synthetic cluster for galaxies of different (absolute) magnitude, without making any distinction according to the morphological type. In Fig. 1a we plot $\sigma^{(n)}$ vs. mag using 0.5-mag bins; it can be seen that the velocity dispersion is roughly independent of magnitude for $M_R > -21.5$ but monotonically decreases at brighter magnitudes, from $\sigma^{(n)} \simeq 1.0\pm0.1$ at $M_R = -21.5$, to $\sigma^{(n)} \simeq 0.3\pm0.3$ at $M_R = -23$. The difference between the velocity dispersions for galaxies brighter and, respectively, fainter than $M_R = -21.5$ is significant at the 0.999 confidence level, according to an F-test.

Galaxies brigther than this magnitude limit are moving more slowly than other cluster galaxies. While it is well known that most cD and D galaxies sit at the bottom of their cluster potential wells, there are at most 31 such galaxies in our sample (see Table 1), as compared to 166 galaxies brighter than $M_R = -21.5$; this effect thus concerns the 4 brightest galaxies of each cluster on average. This segregation in the velocity space may be interpreted as evidence that the brightest cluster galaxies have reached energy equipartition as a consequence of dynamical friction (e.g. Capelato et al. 1981). For a constant galaxy mass-to-light ratio, energy equipartition implies $\sigma \propto 10^{0.2M_R}$. For $M_R \leq -21.5$ this relation is consistent with our data: the regression line between $\log \sigma^{(n)}$ and M_R, has a slope of 0.22 ± 0.06. The same relation (normalized at $M_R = -21.5$) is also shown superposed on the data points in Fig. 1a.

In order to analyse the dependence of luminosity on the galaxy morphological class, we have repeated the previous analysis on the three subsamples of E, S0 and Se+Sl (early- and late-spirals and irregulars are considered together to avoid poor statistics). The σ-magnitude relation for E is similar to that for all galaxies together (see Fig. 2a), and the $\sigma^{(n)}$ of E brighter than $M_R = -21.5$ is significantly lower than the $\sigma^{(n)}$ of fainter E (0.99 confidence level, according to an F-test). On the other hand, this magnitude dependence is not found for the galaxies of other morphological classes.

We then computed $\sigma^{(n)}$ separately for E, S0, Se and Sl of all luminosities (see Fig. 1b). In general, later morphological type galaxies have a larger velocity dispersion than early type galaxies, although there is no significant difference between the S0 and the Se σ. The E σ is 15 % lower than the S0+Se σ, and the latter is 20 % lower than the Sl σ. An F-test qualifies these differences as significant at more than 0.999 confidence level.

We have then considered the Coma (A 1656) cluster independently. In order to achieve a higher signal-to-noise, we used in this case bins of 1 mag, instead of 0.5 mag. We do not need
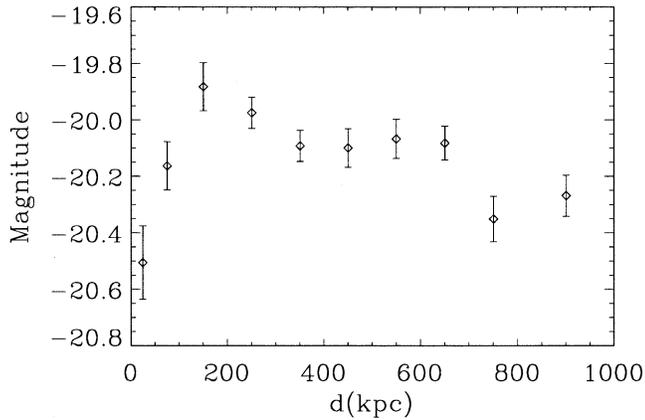
Fig. 4. The average absolute magnitude vs. clustercentric distance (in h^{-1} kpc) for the synthetic cluster

to consider normalized velocities in this case, as all galaxies belong to the same cluster.

Similarly to what was found for the synthetic cluster sample, in the Coma cluster there is evidence for both luminosity and morphology-based segregation in velocity (see Fig. 3). In this case however, the velocity dispersion seems to monotonically increase with magnitude up to the fainter magnitude bin, where $\sigma \simeq 1200$ km s^{-1}. The difference between the σ of galaxies in the brightest magnitude bin and that of galaxies in the adjacent magnitude bin, is consistent with the energy equipartition model, but the global trend is not.

As far as the morphological segregation is concerned, in general later types seem to have larger σ, but the only significant difference is between the σ of E and the σ of other galaxies, in agreement with Andreon (1996).

3.2. Spatial segregation

In the analysis of the spatial segregation, we have to take into account the fact that our sample is not magnitude complete. Magnitude incompleteness is not a problem for the analysis of segregation in velocity, since velocities and magnitudes of cluster galaxies are mostly uncorrelated. On the other hand, observational biases may induce a spurious variation of the average galaxy magnitude with clustercentric distance that may be taken for evidence of spatial luminosity segregation. In particular: (i) the limiting magnitude of galaxies selected for observations with multi-fiber spectroscopy is generally brighter in fields of higher galaxy density (i.e. in the cluster centres); (ii) deep observations generally only cover small fields of view, i.e. the cluster centres and not the wider external regions. Note however that the two biases result in opposite selection effects.

We think that these biases do not seriously affect our analysis for the following reasons: (i) the ENACS sample (which constitutes a large part of our sample) is free of these observational biases (Katgert et al. 1997); (ii) our analysis is limited to the inner cluster regions, where the sampling may be less inhomogeneous; (iii) the combination of several samples is likely

Table 2. Biweight mean clustercentric distances and core-radii r_c, in h^{-1} kpc, of the fitted β models for elliptical (E), lenticular (S0), early spiral (Se) and late spiral galaxies (Sl)

Type	$\bar{d}$	r_c
E	276±11	56±142
S0	373±8	132±111
Se	451±13	159±243
Sl	549±23	197±174

to further reduce the problem, unless all samples are biased the same way.

In Fig. 4 we plot the average magnitude vs. clustercentric distance. Note that the total number of galaxies per bin ranges from 92 to 316, large enough to provide an adequate sampling of the luminosity function at the bright end. Galaxies in the central bin are clearly brighter than those in the adjacent bin. In other bins the magnitude decreases towards the outer parts of the (synthetic) cluster. It is difficult to see how observational biases can produce an artificial decrease of the magnitude with increasing clustercentric distance, while leaving, at the same time, an opposite trend just in the very centre of a cluster. It is possible that a real effect, spatial segregation of the very bright galaxies, is seen superposed on a more general trend that is created by an observational bias. The evidence for spatial segregation must however be considered as tentative only.

For what concerns the morphological segregation, we have considered the distributions of clustercentric distances of E, S0, Se and Sl, separately (see Fig. 5). A Kruskall-Wallis test (see, e.g., Ledermann 1982) indicate that the four distributions are significantly different (>0.999 confidence level). In Table 2 we list the average clustercentric distances of galaxies in the four morphological classes, and the core-radii of the King (1962) functions that best fit the four distributions. Both the average clustercentric distance and the core-radius increase along the Hubble sequence (E-S0-Se-Sl).

Note that the evidence for morphological segregation cannot be accounted for by the trend of galaxy magnitudes with clustercentric distances, since the average magnitudes of E, S0, Se and Sl are similar (-20.2, -20.0, -20.2, -20.0, respectively).

Via the Abel inversion, we have deprojected the King functions to determine the relative fractions of the four morphological types within spheres of given radius; these are plotted in Fig. 6. In Fig. 7 we plot the integrated number of galaxies in each class within a sphere of given radius, normalised to the total number of galaxies in that same class. In addition to the well known morphological segregation between E, S0 and spirals (see, e.g., Whitmore 1994), we also show here the segregation between Se and Sl.

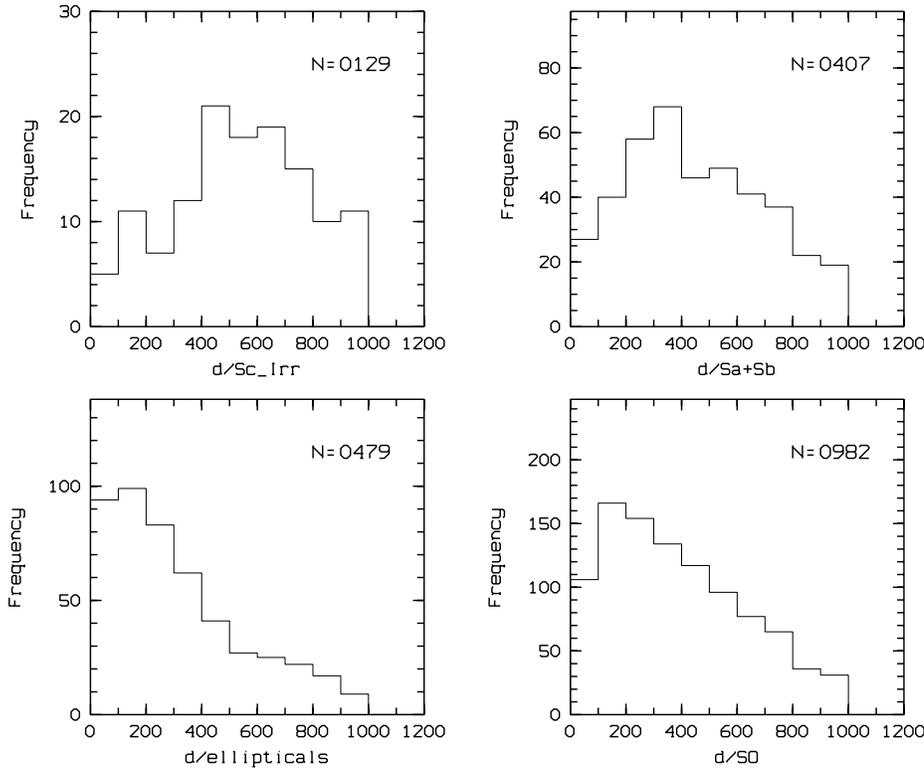We found similar results by considering the Coma cluster sample alone.

Fig. 5. Histograms of the distance from the center in h^{-1} kpc for the four synthetic cluster morphological sub-classes; bottom-left panel: elliptical galaxies, bottom-right panel: S0 galaxies, top-right panel: early spiral galaxies, top-left panel: late spiral galaxies. The number of galaxies in each class is labelled.
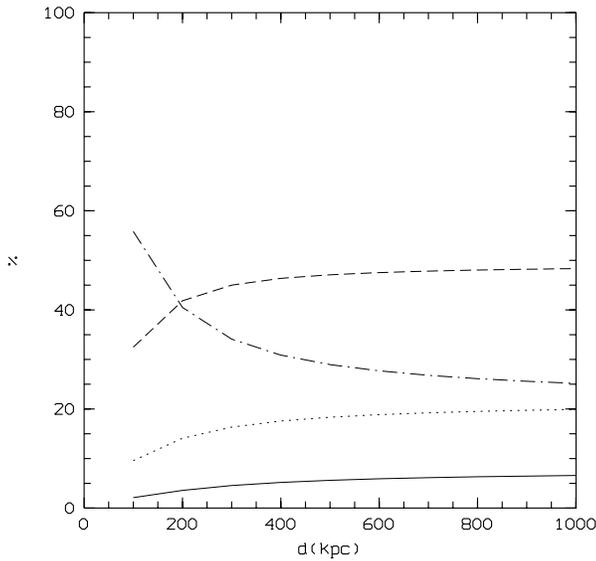

Fig. 6. Percentage fraction of all galaxies in the synthetic cluster per morphological type, within spheres of radii d, in h^{-1} kpc. Solid line: Sl; dotted line: Se; dashed line: S0; dash-dotted line: E.

Fig. 7. Cumulative fraction (in percent) of all galaxies of a given morphological type within spheres of radii d, in h^{-1} kpc. Solid line: Sl; dotted line: Se; dashed line: S0; dash-dotted line: E.

3.3. Phase-space segregation

In the previous sections we have shown that galaxies of different morphological types have different σ (Sect. 3.1) and different spatial distributions (Sect. 3.2). The size of our data-sample allowed us to look for morphological segregation in phase-space, through the determination of the *vdp* of each different morpho-
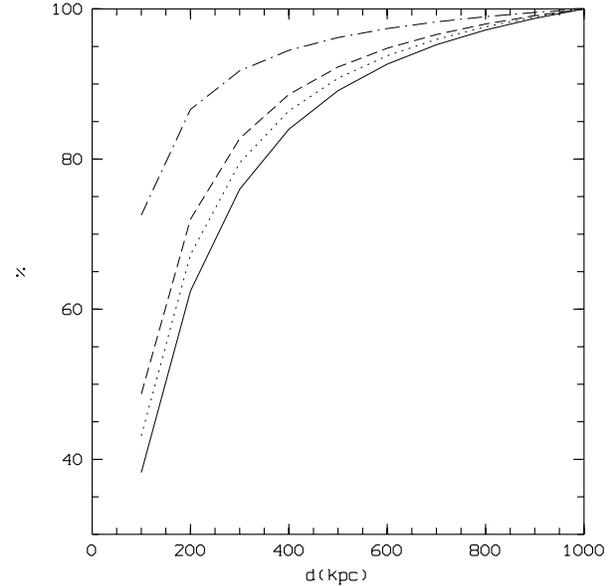
logical class. Each *vdp* was determined using the *LOWESS* technique (Gebhardt et al. 1994; see B97 for a recent application of this technique to galaxy clusters).

In Fig. 8 we plot the *vdp* of all the galaxies of the synthethic cluster, and the *vdp* of E, S0, Se and Sl, separately. Confidence levels are not shown, for clarity, but they are shown in Fig. 9,
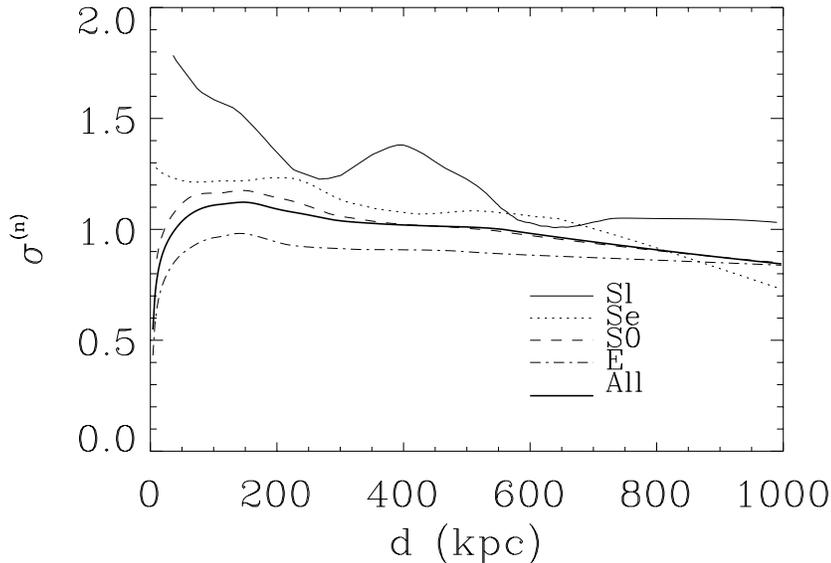
Fig. 8. The velocity dispersion profile of all galaxies (1997) of the synthetic cluster (heavy line), of E only (dash-dotted line), of S0 only (dashed line), of Se only (dotted line) and of Sl only (solid line).

where we plot the *vdp* for each class (with models superposed, see below). The all-galaxy *vdp* is similar to the E-*vdp* and the S0-*vdp* , not surprisingly so, since most cluster galaxies are E and S0. There are notable differences among the *vdp* of the different classes:

- the late-type galaxies have a decreasing *vdp* in the centre, while the early-type galaxies have an increasing *vdp* out to 0.2 h^{-1} Mpc;
- the *vdp* of E, S0 and Se are similar for distances $\geq$ 0.2 h^{-1} Mpc, and nearly flat, while the Sl *vdp* is different and decreasing.

Interpreting these differences requires some modelling of the *vdp* . We have fitted the *vdp* using simple kinematical models in which we take into account the 3D galaxy distribution, as obtained from the King profiles (see Sect. 3.2), and in which we allow the radial velocity profile to vary linearly with clustercentric distance, while the anisotropy, $\mathcal{A} \equiv 1 - (\sigma_t/\sigma_r)^2$, is allowed to vary only when a constant anisotropy model could not provide a reasonable fit.

We found that the steep rise of the E *vdp* requires a substantial degree of tangential anisotropy in the centre ($\mathcal{A} \simeq -7$) and more or less isotropic orbits outside 0.2–0.3 h^{-1} Mpc. The same is true for the S0 *vdp* , although in this case only a modest tangential anisotropy is needed in the cluster centre ($\mathcal{A} \simeq -1$). On the other hand, both the Se and the Sl *vdp* are sufficiently well fitted by constant anisotropy models (with decreasing radial velocity dispersion with radius), with $\mathcal{A} \simeq 0.2$ for Se, and $\mathcal{A} \simeq 0.6$ for Sl.

4. Discussion

Based on a data-set of ~ 2000 galaxies in 40 Abell clusters, we have found that the galaxy phase-space distributions depend on the galaxy morphological types and luminosities. These results are based on a synthetic cluster, generated by combining all available cluster samples, and also on the Coma cluster sample

alone, for which enough data are available to allow such an analysis.

Both the galaxy velocity dispersion and the average cluster-centric distance are smaller, on average, for earlier type galaxies; galaxies brighter than $M_R = -21.5$ have a smaller velocity dispersion than the other cluster galaxies, and the average magnitude of galaxies within 0.1 h^{-1} Mpc from the cluster centre is ~ 0.5 mag lower than the average magnitude of the other cluster galaxies (although the statistical significance of this last result is not well established, as it may be biased by the incompleteness of our sample). Note that the decrease of σ with magnitude only concerns E.

These findings confirm previous ones: the evidence for morphological segregation dates back to Curtis (1918) and Humason et al. (1956), with regards to the spatial distribution, and to Tammann (1972), Melnick & Sargent (1977), and Moss & Dickens (1977) with regards to the velocity distribution. The evidence for luminosity segregation dates back to Rood & Turnrose (1968), with regards to the spatial distribution, and to Rood et al. (1972) with regards to the velocity distribution (see Sect. 1 for reference to more recent works).

The large size of our data-set has allowed us to go beyond these early results and get a better insight into these topics:

1. Within the spiral class, we have considered separately early-spirals and late-spirals + irregulars, and have shown that their distributions are different.
2. We have combined the spatial and velocity distributions to determine the *vdp* of each morphological class, and have shown that they are different.

Modelling of these *vdp* has allowed us to show that the E and S0 orbits are predominantly tangential in the cluster core, and isotropic outside, while Se and Sl orbits have some degree of radial anisotropy (more marked for Sl). The central 3D velocity dispersions (in normalized units) are 1.4, 1.8, 2.1 and 2.4 for E, S0, Se and Sl respectively, and the Sl 3D-σ is larger than the E, S0 and Se 3D-σ at all radii. The Se and Sl *vdp* are steeper than
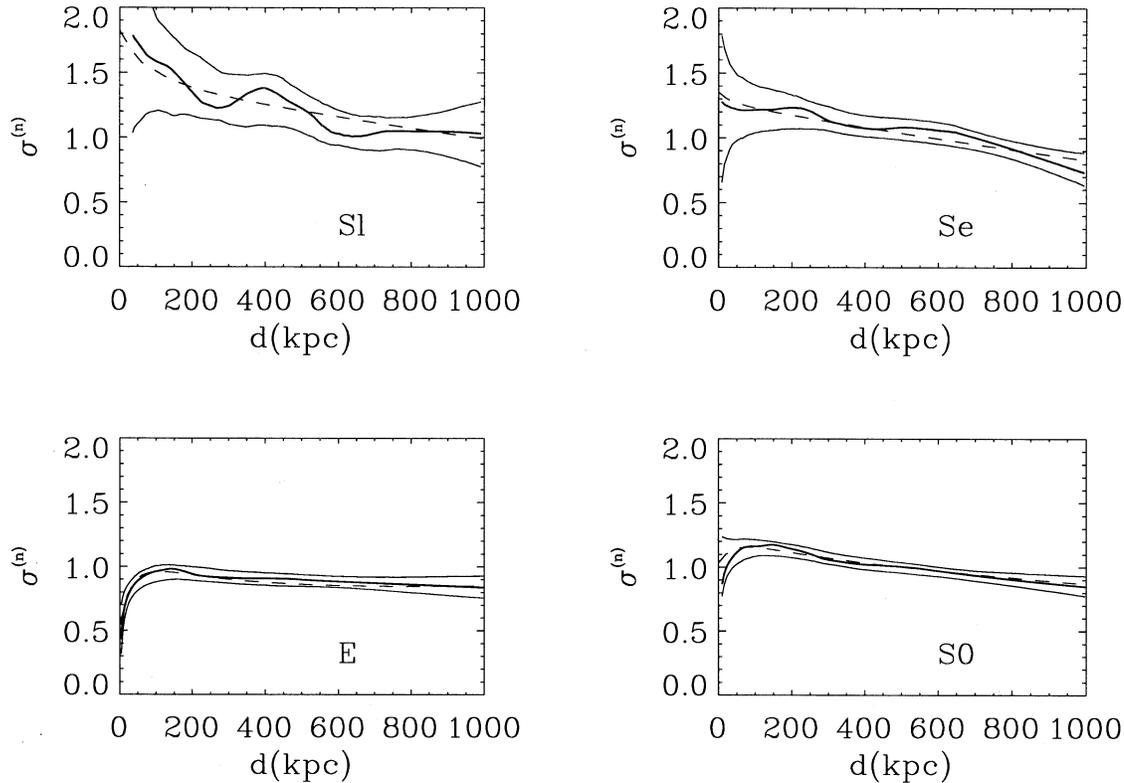
Fig. 9. The velocity dispersion profile of galaxies of a given morphological class (heavy lines) with confidence levels at 90 % (solid lines) and the corresponding best fit models superposed (dashed lines; see text for further details on the models); bottom-left panel: E (479 galaxies); bottom-right panel: S0 (982 galaxies); top-right panel: Se (407 galaxies); top-left panel: Sl (129 galaxies).

the E and S0 *vdp* ; a peaked density profile can produce a steep *vdp* (den Hartog & Katgert 1996), but in our sample we see the opposite, late-type galaxies are characterized by *flatter* density profiles and at the same time *steeper vdp* than early-type galaxies. More likely, the different morphological-type populations do not share the same dynamical status: if S0 are the virialized cluster population, the fact that the Sl kinetic energy is almost twice the S0 kinetic energy in the cluster centre indicates that Sl are a bound yet not virialized cluster population. Their radial anisotropy then suggests that Sl may be falling into the cluster for the first time, similarly to what has been suggested for narrow-angle-tail radio sources (O'Dea et al. 1987). These conclusions recall those of B97 about emission-line galaxies, and those by Tully & Shaya (1984) about spirals in the Virgo cluster.

On the other hand, the low velocity dispersion of E, their tangential anisotropy, and their central location, are all suggestive of a phase-space distribution modified by the process of dynamical friction (den Hartog & Katgert 1996 and references therein). Indeed, if the mass-to-light ratio of cluster galaxies is not a steep function of their luminosities, it is easy to show that the timescale of the dynamical friction process is $\simeq 0.2$ Gyr for $M_R \leq -21.5$ ellipticals in the cluster core (Sarazin 1986). Consistently with this scenario, faint E ($M_R \geq -20$), i.e. those less affected by the process of dynamical friction (assuming they are also less massive), do not share the same *vdp* as bright E,

their orbits being more isotropic and their *vdp* more isothermal (a different kinematics for bright and faint galaxy in the Coma cluster was already suggested by Biviano et al. 1996).

5. Conclusions

Our analysis of the phase-space distributions of ~ 2000 cluster galaxies has shown that they differ according to the galaxy luminosities and morphological types. We have interpreted these differences as evidence that the elliptical phase-space distribution is evolving towards energy equipartition (e.g. Capelato et al. 1981), while, at the other extreme, the late spirals are still falling into the cluster for the first time (e.g. Melnick & Sargent 1977, Moss & Dickens 1977, B97). The phase-space distributions of S0 and early spirals are intermediate between these two extremes.

These findings constrain theories of cluster formation and evolution, as they suggest an ongoing evolution of the cluster population through the process of dynamical friction and of secondary infall. The comparison of the phase-space distributions of distant cluster galaxies with local ones is needed to shed light on this topic. Observations with the *Hubble Space Telescope* (e.g. Dressler & Smail 1997) and/or accurate spectroscopy on 8 m class telescopes should make such a comparison feasible soon.

References

Adami C., Mazure A., Biviano A., Katgert P., Rhee G. 1997a, A&A submitted

Adami C., Mazure A., Katgert P., Biviano A. 1997b, A&A in preparation

Adams M.T., Strom K.M., Strom, S.E. 1980, ApJ 238, 445

Andreon S. 1996, A&A 314, 763

Beers T.C., Bothun G.D. 1992, ApJ 400, 410

Beers T.C., Flynn K., Gebhardt K. 1990, AJ 100, 32

Beers T.C., Forman W., Huchra J.P., Jones C., Gebhardt K. 1991, AJ 102, 1581

Biviano A. 1986, *Laurea* thesis

Biviano A., Durret F., Gerbal D. et al. 1996, A&A 311, 95

Biviano A., Girardi M., Giuricin G., Mardirossian F., Mezzetti M. 1992, ApJ 396, 35 (B92)

Biviano A., Katgert P., Mazure A. et al. 1997, A&A 321, 84 (B97)

Bothun G.D., Schombert J.M. 1988, ApJ 335, 617

Burstein D., Heiles C. 1982, AJ 87, 1165

Butcher H.R., Oemler A.Jr. 1985, ApJS 57, 665
   1980, ApJ 241, 521

Capelato H.V., Gerbal D., Mathez G. et al. 1981, A&A 96, 235

Carlberg R.G., Yee H.K.C., Ellingson E. et al. 1997, ApJ 476, 7

Chapman G.N.F., Geller M.J., Huchra J.P. 1987, AJ 94, 571

Chapman G.N.F., Geller M.J., Huchra J.P. 1988, AJ 95, 999

Chincarini G., Rood H.J. 1977, ApJ 214, 351

Chincarini G., Tarenghi M., Bettis C. 1981, A&A 96, 106

Colless M. 1989, MNRAS 237, 799

Colless M., Dunn A. 1996, ApJ 458, 435

Colless M., Hewett P. 1987, MNRAS 224, 453

Curtis H.D. 1918, Pub. Lick Obs. 13, 55

den Hartog R., Katgert P. 1996, MNRAS 279, 349

Dickens R.J., Currie M.J., Lucey J.R. 1986, MNRAS 220, 679

Dickens R.J., Moss C. 1976, MNRAS 174, 47

Dressler A. 1980a, ApJS 42, 565

Dressler A. 1980b, ApJ 236, 351

Dressler A., Shectman S.A. 1988, AJ 95, 284

Dressler A., Smail I. 1997, in *HST and the High Redshift Universe,* eds. N. Tanvir, A. Aragón-Salamanca, J.V. Wall, World scientific, in press.

Escalera E., Biviano A., Girardi M. et al. 1994, ApJ 423, 539

Ettori S., Guzzo L., Tarenghi M. 1995, MNRAS 276, 689

Faber S.M., Dressler A. 1977, AJ 82, 187

Fabricant D.G., Kent S.M., Kurtz M.J. 1989, ApJ 336, 77

Fabricant D., Kurtz M., Geller M. et al. 1993, AJ 105, 788

Fanti C., Fanti R., Feretti L. et al. 1982 A&A 105, 200

Gavazzi G. 1987, ApJ 320, 96

Gebhardt K., Pryor C., Williams T.B., Hesser J.E. 1994, AJ 107, 2067

Geller M.J., Beers T.C., Bothun G.D., Huchra J.P. 1984, AJ 89, 319

Giovanelli R., Haynes M.P., Chincarini G.L. 1982, ApJ 262, 442

Girardi M., Biviano, A., Giuricin G., Mardirossian F., Mezzetti M. 1993, ApJ 404, 38

Girardi M., Biviano, A., Giuricin G., Mardirossian F., Mezzetti M. 1995, ApJ 438, 527

Girardi M., Fadda D., Giuricin G. et al. 1996, ApJ 457, 61

Gregory S.A., Thompson L.A. 1978, ApJ 222, 784

Gregory S.A., Thompson L.A., Tifft W.G. 1981, ApJ 243, 411

Haynes M.P. 1980, ApJS 42, 83

Hill J.M., Oegerle W. R. 1993, AJ 106, 831

Hintzen P. 1980, AJ 85, 626

Hintzen P., Hill J.M., Lindley D., Scott J.S., Angel J.R.P. 1982, AJ 87, 1656

Hubble E. & Humason M.L. 1931, ApJ 74, 43

Huchra J.P., Geller M.J., Clemens C.M., Tozrk S.P., Michel A. 1995, *The Center for Astrophysics Redshift Catalogue (ZCAT)*

Humason M.L., Mayall N.V., Sandage A.R. 1956, AJ, 61, 144

Katgert P., Mazure A., Perea J. et al. 1996, A&A 310, 8 (K96)

Katgert P., Mazure A., den Hartog R. et al. 1997, A&A submitted

Kent S.M., Gunn J.E. 1982, AJ 87, 945

Kent S.M., Sargent W.L.W. 1983, AJ 88, 697

King, I. 1962, ApJ 62, 471

Lauberts A., Valentijn E.A. 1989 *The Surface Photometry Catalogue of the ESO-Uppsala Galaxies,* Garching bei Munchen: ESO

Lax D. 1985, J.Am.Stat.Assoc. 80, 736

Ledermann W. 1982, *Handbook of Applicable Mathematics,* 6 New York: Wiley

Lucey J.R., Carter, D. 1988, MNRAS 235, 1177

Lucey J.R., Dickens R.J., Mitchell R.J., Dawe J. A. 1983, MNRAS 203, 545

Lugger P.M. 1989, ApJ 343, 572

Malumuth E.M., Kriss G.A., Van Dyke Dixon W., Ferguson H.C., Ritchie C. 1992, AJ 104, 495

Mamon G.A. 1992, ApJ 401, 1

Mamon G.A. 1996, in "Third Chalonge Colloque Cosmologie", p.95, H. de Vega, N.S. Sánchez eds. (Singapore: World Scientific) (astro-ph/9511101)

Melnick J., Sargent W.L.W. 1977, ApJ 215, 401

Mohr J.J., Geller M.J., Fabricant D.G. et al. 1996, ApJ 470, 724

Moss C., Dickens R.J. 1977, MNRAS 178, 701

Nilson P. 1973, *Uppsala General Catalogue of Galaxies,* Stockholm, Almquist and Wiksell

O'Dea C.P., Sarazin C.L., Owen F.N. 1987, ApJ, 316, 113

Oegerle W.R., Hoessel J.G. 1989, AJ 98, 15230

Oemler A. Jr. 1974, ApJ 194, 1

Oemler A. Jr. 1992, in "Clusters and Superclusters of Galaxies", p.29, A. Fabian ed. (Dordrecht: Kluwer Academic Publishers)

Ostriker E.C., Huchra J.P., Geller M.J., Kurtz M.J. 1988, AJ 96, 1775

Pinkney J., Rhee G., Burns J.O. 1993, ApJ 416, 36

Postman M., Lauer T. R. 1995, ApJ 440, 28

Poulain P., Nieto J.L., Davoust E. 1992, A&AS 95,129

Proust D., Quintana H., Mazure A. et al. 1992, A&A 258, 243

Quintana H., Ramirez A. 1990, AJ 100, 1424

Richter O.G. 1987, A&AS 67, 237

Richter O.G. 1989, A&AS 77, 237

Rood H.J., Page T.L., Kintner E.C., King I.R. 1972, ApJ, 175, 627

Rood H.J., Turnrose B.E. 1968, ApJ 152, 1057

Sandage A. 1973, ApJ 183, 711

Sanromà M., Salvador-Solé E. 1990, ApJ 360, 16

Sarazin C.L. 1986, Rev. Mod. Phys. 58, 1

Schneider D.P., Gunn J.E., Hoessel J.G. 1983, ApJ 264, 337

Scodeggio M., Solanes J.M., Giovanelli R., Haynes M.P. 1995, ApJ 444, 41

Sharples R.M., Ellis R.S., Gray P.M. 1988, MNRAS 231, 479

Sodré L.Jr., Capelato H.V., Steiner J.E., Mazure A. 1989, AJ 97, 1279

Stein P. 1996, A&AS 116, 203

Stein P. 1997, A&A 317, 670 (S97)

Struble M.F. 1979, AJ 84, 27

Tammann G.A. 1972, A&A 21, 355

Tarenghi M., Tifft W. G., Chincarini G., Rood H.J., Thompson L.A. 1979, ApJ 234, 793

Teague P.F., Carter D., Gray P.M. 1990, ApJS 72, 715

Tifft W.G. 1978, ApJ 222, 54

Tully R.B., Shaya E.J. 1984, ApJ 281, 31

White S.D.M. 1992, in "Clusters and Superclusters of Galaxies", p.17, A. Fabian ed. (Dordrecht: Kluwer Academic Publishers)

Whitmore B.C. 1994, in "Clusters of Galaxies", proc. of the XXIX Rencontre de Moriond, p.69, F. Durret, A. Mazure, J. Trân Thanh Vân eds. (Singapore: Editions Frontières)

Whitmore B.C., Gilmore D.M. 1991, ApJ 367, 94

Whitmore B.C., Gilmore D.M., Jones C. 1993, ApJ, 407, 489

Willmer C.N.A., Focardi P., Chan R., Pellegrini P.S., Nicolaci Da Costa L. 1991, AJ 101, 57

Yepes G., Dominguez-Tenreiro R., Del Pozo-Sanz R. 1991, ApJ 373, 336

Zabludoff A.I., Geller M.J., Huchra J.P., Vogeley M.S. 1993, AJ 106, 1273

Zabludoff A.I., Huchra J.P., Geller M.J. 1990, ApJS 74, 1

Zwicky F., Herzog E., Wild P., Karpowicz M., Kowal C. 1961-1968 *Catalog of Galaxies and of Clusters of Galaxies,* vol.s 1-6, Pasadena: California Institute of Technology